Quantitative measurements of indentation moduli by atomic force acoustic microscopy using a dual reference method

Gheorghe Stan[a)] and William Price

Materials Science and Engineering Laboratory, National Institute of Standards and Technology,
100 Bureau Drive, Gaithersburg, Maryland 20899

Atomic force acoustic microscopy (AFAM) was used to quantitatively determine material indentation moduli by measuring local mechanical responses. A dual reference method has been shown to be capable of extracting the modulus of a material within 3% of the calculated expected value without any assumptions of the probe's mechanical properties. The use of this developed method also allows for the calculation of the maximum precision in the quantitative determination of the indentation modulus of materials using AFAM. A parallel analysis of the single and dual reference AFAM techniques isolates the inaccuracy induced by the assumption that the indentation modulus of the atomic force microscopy probe used is the same as bulk silicon. [DOI: 10.1063/1.2360971]

I. INTRODUCTION

Since the introduction of modulation in the ultrasonic frequency range to obtain material properties,[1,2] attempts have been made to quantify the measurements. As with any atomic force microscopy (AFM) based technique, knowledge of the probe composition, dimension, and mechanical properties has always been required prior to modeling and quantifying results from experimental data. In many reported papers, researchers have taken care to analyze tip contact geometry via scanning electron microscopy (SEM),[3,4] and have used reference materials[5–7] to address irregularities in measurements. Unfortunately, direct measurements of the mechanical properties of the probe are not trivial and many researchers assume bulk property values for the probe. These assumptions, in combination with the use of only one reference material [atomic force acoustic microscopy (AFAM) single reference method] and individual measurements on materials, can lead to errors of 20% or more[5,8] in the determination of the indentation modulus.

The idea of using two reference materials (dual reference method) was originally reported by Rabe *et al.*[6,7] Building on this idea we have introduced a rigorous method of data acquisition and analysis to determine quantitatively the indentation modulus of homogeneous materials. The method introduced in this article eliminates the need for two of the most common and ambiguous assumptions made when using a scanning probe method: the properties of the probe and the tip-surface contact radius. Using a parallel analysis of the measurements with both single and dual reference methods we identified a major source of inaccuracy in the AFAM single reference method to be the uncertainty in the assumed value for the indentation modulus of the tip used.

Using the method presented here the indentation modulus of several single-crystal materials has been determined to within 3% of the theoretical values. The dual reference method has proven effective for measuring the mechanical properties of a variety of materials. A selection guide for choosing adequate reference materials to achieve the best measurement precision for a given unknown material has also been developed.

II. MATERIALS AND EXPERIMENTAL METHODS

The materials[9] used were single crystals of $CaF_2(100)$ and $MgF_2(001)$ from CVI Laser Optics and Si(100) from Virginia Semiconductor. In addition, a 300 nm thick Au(111) film epitaxially grown on mica was acquired from Georg Albert PVD-Beschichtungen. All of the samples used had a rms roughness of 1.2–1.6 nm as measured by AFM. AFAM instrumentation[9] included a Veeco DI Multimode AFM and silicon AFM probes MPP-23100. The AFM probes used are phosphorus (n) doped Si, 225 μm in length, 40 μm in width, 7 μm in thickness and have a force constant of 35 N/m, as reported by the manufacturer. A lock-in amplifier, Signal Recovery 7280, was used to generate the signal driving the cantilever and acquire the photodiode signal. In addition custom software was programmed using National Instruments LABVIEW to synchronize acquisition of cantilever spectra while scanning the surface. Data were subsequently analyzed in WaveMetrics IGOR PRO to extract the contact resonance frequency and perform statistical analysis. The contact resonance spectra were acquired with a 2.4 μN applied load and a cantilever oscillation amplitude of 0.7 nm.

AFAM measurements, as with many nanoscale contact interactions, are very sensitive to contact area changes. In addition to the use of smooth sample surfaces, care was taken to track any changes that occur[5] and ensure that measurements are acquired with a stable tip geometry. After preliminary scans, which produced a stable flattened tip, spectra were obtained in a sample order of MgF_2, CaF_2, Au, and Si, twice, starting and ending with the stiffest materials to ensure

---

a)Electronic mail: gheorghe.stan@nist.gov
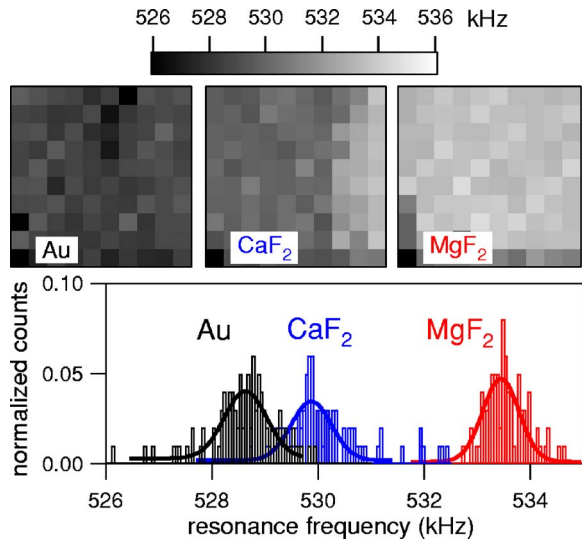
FIG. 1. (Color online) The first contact resonance frequencies measured over 3×3 μm^2 areas of the Au, CaF_2, and MgF_2 samples. In the bottom plot are shown the histograms made with the measured values shown in the top panel.

no systematic errors based on the sample order were introduced into the analysis. The reproducibility and stability of the tip-surface contact resonance spectra were checked by acquiring data over a 10×10 array of points on a 3×3 μm^2 surface. At each grid node, spectra centered on the first and second contact resonance frequencies were acquired with 100 kHz bandwidth. A delay of 1 s was imposed between measurements to allow for the damping of vibrations induced by the movement of the cantilever across the surface.

III. RESULTS AND DISCUSSION

Figures 1 and 2 show the distributions of the first and second contact resonance peaks acquired for Au(111), CaF_2(100), and MgF_2(001). A Gaussian fit of each histogram was used to determine the most probable contact resonance
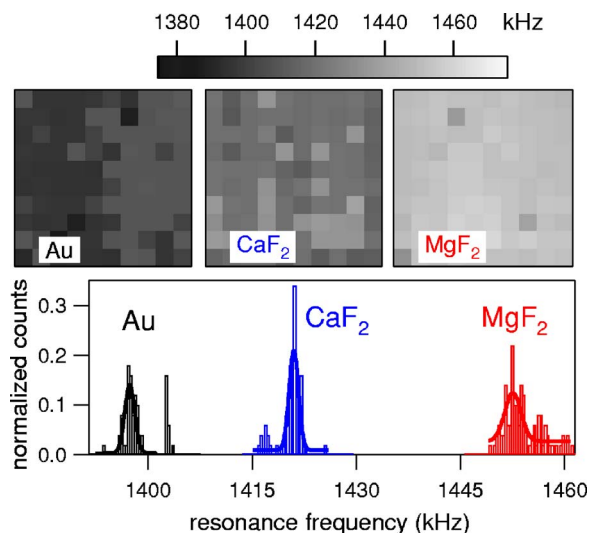
FIG. 2. (Color online) The second contact resonance frequencies measured over the same areas shown in Fig. 1. In the bottom plot are shown the histograms made with the measured values shown in the top panel.

TABLE I. First and second measured contact resonances.

Material	First contact resonance (kHz)	Second contact resonance (kHz)
MgF_2(001)	533.44 ± 0.34	1452.05 ± 1.17
CaF_2(100)	529.87 ± 0.37	1421.00 ± 0.68
Au(111)	528.63 ± 0.39	1397.35 ± 0.71
Si(100)	533.95 ± 0.24	1452.40 ± 1.32

frequency and the full width at half maximum of the data was used to estimate the uncertainty with the results presented in Table I. In general, the measured contact resonance frequencies show statistical variation around the averaged values. The apparent anomalies along the right side of CaF_2 and the bottom row of MgF_2 (Fig. 1) are only transient observations and do not recur in subsequent measurements across the same surface. These data points have been included to show how single AFAM measurements may occur well outside of a normal distribution and stress the need for the use of a sampling array for quantitative indentation moduli measurements with the AFAM technique. The first and second free resonances of the cantilever in air are 113.91 ± 0.01 and 725.62 ± 0.01 kHz, respectively.

The shift in the resonance frequency of the cantilever from air to contact is quantified in terms of the contact stiffness between the AFM probe and the sample. The cantilever-beam model[8,10,11] for small amplitude vibrations has been used to calculate the normal contact stiffness k^*. Consideration for the lateral contact stiffness k_l^*, the cantilever tilt α $=11°$, and the tip position along the cantilever beam λ $=L/L_0$ has been included in the calculations. L is the tip position from the cantilever's base and L_0 is the total cantilever length.

In the case of a circular contact area of radius a, the ratio between the normal contact stiffness k^* and the contact diameter gives the reduced indentation modulus E^* of the material[12]

$$E^* = k^*/2a. \tag{1}$$

The contact radius a is further related to the normal contact stiffness depending on the particular geometry of the contact.[12] The relationship between k^* and E^* is linear for a flat punch on a planar surface[5] but follows a 3/2-power law in the case of Hertzian contact between a spherical tip and a planar surface.[12] The effect of tip geometry on the calculation of the indentation modulus of materials with AFAM will be considered in the subsequent discussion.

A standard AFAM procedure in determining the indentation modulus of a sample is to report the ratio of the normal contact stiffnesses measured on that sample k_S^* and the normal contact stiffness measured on a known reference material k_R^*.[5] This connects the reduced modulus of the sample E_S^* to the reduced modulus of the reference material E_R^*,

$$E_S^* = E_R^*(k_S^*/k_R^*)^n, \tag{2}$$

where $n=1$ for a flat tip and $n=3/2$ for a spherical tip in contact with a planar surface. The reduced indentation modulus of two bodies in contact can be calculated by

$$1/E^* = 1/M_S + 1/M_T, \tag{3}$$

where M_S and M_T are the indentation moduli of the sample and the tip, respectively.[13] By combining Eqs. (2) and (3), the indentation modulus of the sample is expressed as

$$1/M_S = (k_R^*/k_S^*)^n/M_R + [(k_R^*/k_S^*)^n - 1]/M_T. \tag{4}$$

Implicit in these calculations is that the tip is considered as a second reference material and assumed to have the same indentation modulus as the bulk material of which it is composed. Since the mechanical properties of the silicon tip during scans could be altered by the SiO_2 network over the surface of the tip[16] and the amorphous regions induced as a result of nanodeformation,[17] the validity of this assumption is called into question.

The use of the dual reference method eliminates the need for any assumption of the indentation modulus of the tip. In this method, the indentation moduli of the two reference materials M_{R1} and M_{R2} and their normal contact stiffnesses k_{R1}^* and k_{R2}^*, respectively, and the normal contact stiffness of the sample k_S^* are measured with the same AFM probe and used to calculate the indentation modulus of the sample M_S:

$$M_S = \frac{(k_{R1}^*/k_{R2}^*)^n - 1}{(k_{R1}^*/k_S^*)^n[(1/M_{R2}) - (1/M_{R1})] + (k_{R1}^*/k_{R2}^*)^n(1/M_{R1}) - (1/M_{R2})}. \tag{5}$$

Theoretical values for the indentation modulus of the materials used in this experiment are calculated for an axisymmetric indenter on a half-space anisotropic crystal[14] using elastic constants reported for these materials.[15]

The validity of this method was checked by using as references the theoretical values for each pair of the four materials studied. The moduli of the other two materials were then calculated using Eq. (5) for every pair. The contact resonances of MgF_2 and Si overlapped, eliminating the use of this pair of materials as references.

In Table II the indentation moduli have been calculated with the dual reference method for the investigated materials by considering both a flat and a spherical tip. Other variables in these calculations included the tip height $h = 17$ μm, cantilever length $L = 225$ μm, and $\lambda = 1.00$ (from which k_l^*/k^* is calculated to be in the range of 0.7–1.0). The tip's height and length are vendor supplied values. The tip position parameter λ was determined from SEM images which show that the square pyramidal tip is located at the end of the cantilever, and the end of the cantilever is etched around the tip.

Calculations were performed to determine the contribution of the coupling ratio k_l^*/k^* and the tip's position parameter λ to the normal contact stiffness k^* of each tested material. Using the cantilever-beam model[8,10,11] for a given value of k_l^*/k^* and the two measured contact frequencies, k^* and λ are simultaneously determined. When the coupling ratio k_l^*/k^* was varied between 0.0 and 1.0, λ was calculated in the range of 0.96–1.00. Across the four materials λ was found to vary within 1% for each value of the coupling ratio. This calculation also supports our ascertainment of a stable contact geometry during the measurements. These variations of k_l^*/k^* and λ marginally affect the values of the material indentation moduli calculated in the dual reference method with deviations of 1%–2% of the values shown in Table II. In general, as can be seen in Table II, the deviations from the theoretical values of the calculated indentation moduli are in the range of 2%–3% and the material indentation moduli determined with this dual reference method are insensitive to the tip's shape (flat or spherical).

A by-product of this dual reference method permits the calculation of the indentation modulus of the tip[7]

$$M_T = \frac{[(k_{R1}^*)^n - (k_{R2}^*)^n]M_{R1}M_{R2}}{(k_{R2}^*)^n M_{R1} - (k_{R1}^*)^n M_{R2}}. \tag{6}$$

For this calculation we have considered three possible tip positions, $\lambda = 0.964$, 0.980, and 1.000. From these the ratio of lateral to normal contact stiffness was calculated along with the indentation moduli for the tip considering flat contact $n = 1$, and spherical contact geometries, $n = 3/2$, with the results presented in Table III. In stark contrast to the calculations of the indentation moduli of the sample M_S, M_T is extremely sensitive to the parameters of tip position λ, contact geometry n, and lateral coupling k_l^*/k^*. The large variability in M_T, from 45 to 120 GPa for a flat tip and from 80 to 350 GPa for a spherical tip, shows that the current theoretical models for flat or spherical tips do not comprise an

TABLE II. Indentation modulus (in GPa) of the materials measured. Theoretical values are included in parentheses. For every other row, each experimental value is determined by considering the two checked materials as references.

Au(111) (99.7)	CaF$_2$(100) (124.5)	Si(100) (164.8)	MgF$_2$(001) (167.8)
⋯	⋯	181.2±4.1[a]	180.1±4.0[a]
⋯	120.8±0.7[a]	⋯	164.0±3.3[a]
⋯	121.7±0.7[a]	168.6±3.6[a]	⋯
104.2±0.8[a]	⋯	⋯	164.1±2.9[a]
103.1±0.9[a]	⋯	168.6±3.3[a]	⋯
⋯	⋯	176.8±3.6[b]	175.9±3.6[b]
⋯	121.6±0.7[b]	⋯	164.1±3.1[b]
⋯	122.6±0.8[b]	168.6±3.4[b]	⋯
103.3±0.8[b]	⋯	⋯	164.1±2.8[b]
102.1±0.9[b]	⋯	168.5±3.2[b]	⋯

[a]Flat tip geometry.
[b]Spherical tip geometry.

TABLE III. Calculated indentation modulus for the Si tip.

λ	k_l^*/k^*	$M_T(n=1)$	$M_T(n=3/2)$
0.964	0	45–55	80–100
0.980	0.3–0.4	60–85	140–180
1.000	0.7–1.0	80–120	190–350

accurate description for AFM probes used in our AFAM measurements.

Using the commonly assumed value of 165 GPa for M_T, from single-crystal Si(100), a spherical tip geometry would make sense in Table III, with $\lambda=0.98$ and $k_l^*/k^*=0.3-0.4$. However, the preliminary scans employed in this method which assure a subsequent stable contact geometry, flattened the end of the tip. This is visible in the SEM images of our used tip (Fig. 3). Detailed investigations[3,4] on used AFM tips clearly show in some cases that the end of the tip has been flattened and can no longer be considered spherical. For our experiments, with a flat tip located near the end of the cantilever, M_T is calculated to be around 100 GPa (see Table III), which is comparable to silicon oxide films on Si substrate[18] or with that of the amorphous silicon.[19] Since the oxidation of silicon tips have been investigated in detail,[16] the formation of amorphous Si at the end of the Si(100) tips used can be rationalized considering the high contact pressures that occur during the initial contact scans which flatten the tip. The dislocated material that piles up at the end of the tip is likely to be amorphous Si similar to the extruded material observed in indentations made on single-crystal Si.[17,20]

In contrast with the dual reference method, the single
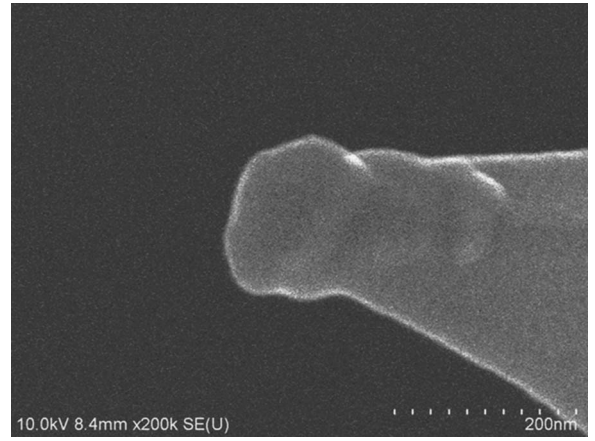
FIG. 3. SEM image of the AFM probe after AFAM measurements.

reference method has been shown to produce accurate results only if the chosen reference material is close, in terms of mechanical properties, to the tested material.[21] Under these conditions, the last term in Eq. (4) is negligible and the error which arises from any assumed value for the indentation modulus of the tip is reduced. However, any variation ΔM_T in the tip's indentation modulus from the assumed value $M_{Si(100)}=164.8$ GPa affects the measured ratio of the contact stiffnesses

$$\frac{k_R^*}{k_S^*} = \frac{M_R\{M_S + [M_{Si(100)} + \Delta M_T]\}}{M_S\{M_R + [M_{Si(100)} + \Delta M_T]\}}. \quad (7)$$

When Eq. (4) is used with $M_T=M_{Si(100)}$ where the real value actually is $M_T=M_{Si(100)}+\Delta M_T$, the indentation modulus of the tested material M_S will be off by

$$\Delta M_S = \frac{1}{[M_R(M_S+M_{Si}+\Delta M_T)/M_S(M_R+M_{Si}+\Delta M_T)]^n[(1/M_R)+(1/M_{Si})] - \frac{1}{M_{Si}}} - M_S. \quad (8)$$

The inaccuracy introduced into the AFAM single reference method by the uncertainty in the indentation modulus of the tip is shown graphically in Fig. 4 as a function of the indentation modulus of the reference material. The tested materials considered are Au(111) in Fig. 4(a) and Si(100) in Fig. 4(b) and the reference material has an indentation modulus in the range of 50–250 GPa. The possible values for the Si flat tip have been considered in the range of 100–200 GPa. As can be seen, ΔM_S is small when the reference material has an indentation modulus close to that of the tested material, regardless of any uncertainty in the indentation modulus of the tip. If, however, the indentation modulus of the reference material is different from that of the tested material any deviation of the tip's indentation modulus from the assumed value of 164.8 GPa will introduce significant errors into the calculation of the indentation modulus of the tested material.

The dependence of the deviation ΔM_S on the reference materials cannot be explained consistently by inaccuracies in the indentation moduli of the considered reference materials. The experimentally observed sensitivity to the chosen reference material is a result of the uncertainty in equating the mechanical properties of the tip to single-crystal bulk silicon.

Using the AFAM single reference method and our experimental results, assuming $M_T=164.8$ GPa, $M_{Au(111)}$ would be off by 6.4 ± 0.5 GPa when CaF_2 is used as reference and 9.5 ± 1.3 GPa when Si is considered as reference. Correlating these results with Fig. 4(a), ΔM_S for $M_{Au(111)}$ is 4.5 GPa when CaF_2 is the reference material and 10 GPa when Si is the reference. These values indicate that the tip used in our measurements has an indentation modulus of 100 GPa.

With the dual reference method, M_T is not used and the indentation moduli of the measured materials are only marginally affected by the contact geometry. For example, the
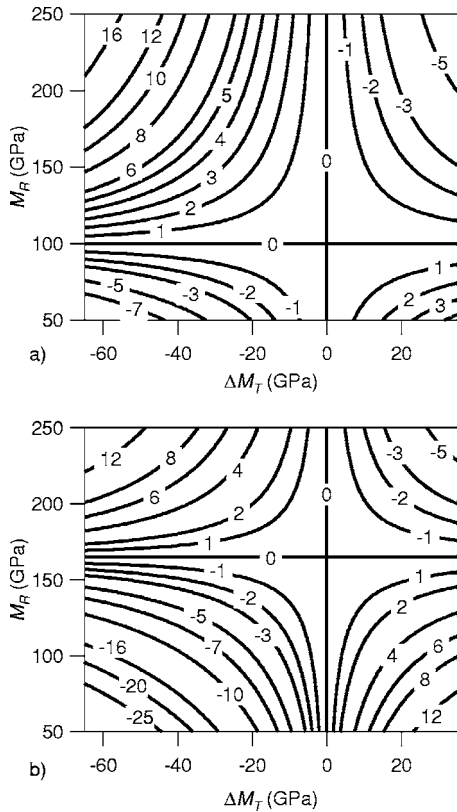
FIG. 4. The inaccuracy in the indentation modulus of the tested material ΔM_S induced in the AFAM single reference method by the uncertainty in the tip's indentation modulus ΔM_T. The tested material is (a) Au(111) and (b) Si(100). The contour labels are in GPa.

FIG. 5. [(a) and (b)] The theoretical uncertainty ΔM_S in measuring the indentation modulus M_S of Si(100) with the dual reference method (see text for details). Choosing two references that bracket Si results in an uncertainty of 3 GPa or less (gray areas). (c) Cross sections of (a) (continuous line) and (b) (dashed line) for $M_{R1} = 100$ GPa.

indentation modulus of gold with CaF_2 and Si as references was off only by 3.6 ± 0.8 GPa from its theoretical value (see Table II). Furthermore, the uncertainty of the method is determined only by the chosen reference materials. In Fig. 5 the uncertainty in the AFAM dual reference method is shown for Si(100). In Fig. 5(a) the uncertainty ΔM_S has been calculated from the linear-squares regression fitting of the points $(M_{R1}, M_{R1} \pm \Delta M_{R1})$, $(M_{R2}, M_{R2} \pm \Delta M_{R2})$, and $(M_S, M_S \pm \Delta M_S)$,

$$\Delta M_S = \Delta M_{R1} \left| \frac{M_S - M_{R2}}{M_{R2} - M_{R1}} \right| + \Delta M_{R2} \left| \frac{M_S - M_{R1}}{M_{R2} - M_{R1}} \right|, \quad (9)$$

whereas in Fig. 5(b) the summing in quadrature has been used to estimate ΔM_S from Eq. (5),

$$\Delta M_S = \sqrt{\left(\frac{\partial M_S}{\partial M_{R1}} \right)^2 (\Delta M_{R1})^2 + \left(\frac{\partial M_S}{\partial M_{R2}} \right)^2 (\Delta M_{R2})^2}. \quad (10)$$

ΔM_{R1} and ΔM_{R2} are calculated considering the frequency resolution[8] for the second mode of a 35 N/m cantilever as 1.0% of the first free resonance (appropriate values for our experiment). The tip was assumed to be flat with $M_T = 100$ GPa and contact radius of 40 nm. Both calculation methods give similar results for quite a large range around the tested material.

As can be seen, the best measurement precision is obtained when the two reference materials bracket the tested material. The largest uncertainty, a worst case scenario, would be to have two references, each with similar mechani-

cal properties but different from those of the tested material. These results have been confirmed quantitatively by our measurements for the tested materials, as can be easily seen in Fig. 5(c) with Au as one of the reference material for the measurement of the indentation modulus of the Si(100). It is worth noting that the calculated uncertainty ΔM_S in the dual reference method is only marginally affected by the mechanical properties of the tip. It is primarily determined by the mechanical properties of the two chosen reference materials. Therefore, the calculation of ΔM_S constitutes a selection rule for the two reference materials that are appropriate for measuring a given material.

IV. SUMMARY

The dual reference AFAM method has been shown capable of extracting the modulus of a material within 3% of the calculated expected values. The analysis method described here requires no assumptions of the material or the mechanical properties of the AFM probe. As a beneficial side effect this dual reference method is insensitive to the tip's

shape (flat or spherical), the tip's position λ, or the ratio of the contact coupling strength (k_l^*/k^*). Single-crystal or aligned samples with well-characterized moduli are used as reference samples and the measurement precision can be controlled by an adequate selection of the two reference materials. Although this method is more rigorous experimentally, it eliminates the need for *a priori* knowledge of the mechanical properties of the sample investigated, or the AFM probe used. The dual reference has been proven theoretically and experimentally to be more accurate than the single reference method.

ACKNOWLEDGMENTS

[1] U. Rabe and W. Arnold, Appl. Phys. Lett. **64**, 1493 (1994).
[2] K. Yamanaka, H. Ogiso, and O. Kolosov, Appl. Phys. Lett. **64**, 178 (1994).
[3] D. Passeri, A. Bettuci, M. Germano, M. Rossi, A. Alippi, S. Orlanducci, M. Terranova, and M. Ciavarella, Rev. Sci. Instrum. **76**, 093904 (2005).
[4] M. Kopycinska-Muller, R. C. Geiss, and D. C. Hurley, Ultramicroscopy **107**, 466 (2006).
[5] U. Rabe, S. Amelio, M. Kopycinska, S. Hirsekorn, M. Kempf, M. Goken, and W. Arnold, Surf. Interface Anal. **33**, 65 (2002).
[6] U. Rabe, M. Kopycinska, S. Hirsekorn, J. Muñoz Saldaña, G. A. Schneider, and W. Arnold, J. Phys. D **35**, 2621 (2002).
[7] *Applied Scanning Probe Methods*, edited by B. Bushan and H. Fuchs (Springer, New York, 2006), Vol. II.
[8] U. Rabe, S. Amelio, E. Kester, V. Scherer, S. Hirsekorn, and W. Arnold, Ultrasonics **38**, 430 (2000).
[9] Certain commercial equipment, instruments, or materials are identified in this article to adequately specify the experimental procedure. Such identification is not intended to imply recommendation or endorsement by the National Institute of Standards and Technology, nor is it intended to imply that the materials or equipment identified are necessarily the best available for the purpose.
[10] U. Rabe, K. Janser, and W. Arnold, Rev. Sci. Instrum. **67**, 3281 (1996).
[11] E. Dupas, G. Gremaud, A. Kulik, and J.-L. Loubet, Rev. Sci. Instrum. **72**, 3891 (2001).
[12] K. L. Johnson, *Contact Mechanics* (Cambridge University Press, Cambridge, 1995).
[13] G. M. Pharr, W. C. Oliver, and F. R. Brotzen, J. Mater. Res. **7**, 613 (1992).
[14] J. J. Vlassak and W. D. Nix, J. Mech. Phys. Solids **42**, 1223 (1994).
[15] H. M. Kandil, J. D. Greiner, A. C. Ayers, and J. F. Smith, J. Appl. Phys. **52**, 759 (1981); C. R. A. Catlow, J. D. Comins, F. A. Germano, R. T. Harley, and W. Hayes, J. Phys. C **11**, 3197 (1978); J. R. Neighbours and C. A. Alers, Phys. Rev. **11**, 707 (1958); W. P. Mason, *Physical Acoustics and Properties of Solids* (Van Nostrand, New York, 1958).
[16] K.-H. Chung, Y.-H. Lee, and D.-E. Kim, Ultramicroscopy **102**, 161 (2005).
[17] I. Zarudi, J. Zou, and L. C. Zhang, Appl. Phys. Lett. **82**, 874 (2003).
[18] M. T. Kim, Thin Solid Films **283**, 12 (1996).
[19] C. Gaire, D.-X. Ye, F. Tang, R. C. Picu, G.-C. Wang, and T.-M. Lu, J. Nanosci. Nanotechnol. **5**, 1893 (2005).
[20] J.-I. Jang, M. J. Lance, S. Wen, T. Y. Tsui, and G. M. Pharr, Acta Mater. **53**, 1759 (2005).
[21] D. C. Hurley, K. Shen, N. M. Jennett, and J. A. Turner, J. Appl. Phys. **94**, 2347 (2003).